Nottingham effect's impact on the heating of nanoscale surface defects

University of Tartu

Kristjan Eimre
Supervisor Vahur Zadin

May 07, 2014

Contents

Abbrevations and symbols

Greek letters

$\varphi(\boldsymbol{r})$	Electric potential
$\rho(\boldsymbol{r})$	Space charge density
ϵ_0	Electric constant
$\mathcal{E}$	Electric field??? NOPE, use E

1. Introduction

Paljudes tänapäevastes rakendustes kasutatakse kõrgeid elektrivälju, millega kaasnevad elektrilised läbiöögid. Nende läbilöökide tagajärjel võivad seadmed kahjustuda. CERN-is välja töötatava lineaarkiirendi CLIC [1] puhul on nende läbilöökide kontrolli alla saamine otsustava tähtsusega.

Kõrgete elektriväljadega kaasnevad emissioonivoolud, mis soojendavad materjali. Käesolevas töös lisatakse Nottinghami efekti mõju materjali soojustasakaalu mudelile. Protsessi simuleeritakse lõplike elementide meetodil, kasutades programmipaketti *Comsol Multiphysics* [2].

Overview of CLIC and the essence of breakdowns.

The goals/objectives of this work.

1.1 Background

What has been done previously in the field?

1.2 Scope

1.3 Outline

2. Literature overview

2.1 Thermionic emission

General information about electron emission, more citations about emission equations (see for example Jensen2007 introduction). Also citation ranges.

What energy barrier at the surface? Only height is needed and $\Phi - \sqrt{\frac{q^2F}{4\pi\epsilon_0}}$ is the height of Schottky barrier.

Thermionic emission is the dominant contributing effect to emission current under relatively low field and high temperature conditions (see section 2.3). It is usually characterised by the Richardson-Schottky equation [3, 4]

$$J_T(F,T,\Phi) = A_{RLD}T^2 \exp\left(\frac{-\Phi + \sqrt{\frac{q^2F}{4\pi\epsilon_0}}}{k_BT}\right), \tag{2.1}$$

where J_T is the thermionic emission current density, F is the product of local electric field and the elementary charge change to E?, T is temperature, Φ is the work function, $A_{RLD} = \frac{4\pi m k_B^2 q}{h_P^3}$ is Richardson's constant, m is the mass of an electron, k_B is the Boltzmann's constant, q is the elementary charge, h_P is the Planck's constant and ϵ_0 is the electric constant.

2.2 Field emission

Under relatively low temperature and high field conditions (see section 2.3), the dominant electron emission effect is field emission. In the current work, metal surfaces are assumed to obey the Schottky-Nordheim surface energy barrier [5]

$$V_{SN}(F_e,h,x) = h - qF_ex - \frac{q^2}{16\pi\epsilon_0 x}, \tag{2.2}$$

where V_{SN} is the potential energy, F_e is the local electric field[1], h is the unreduced height of the energy barrier (in our case $h = \Phi$, where Φ is the work function) and x is a coordinate,

[1]The used symbols correspond to the ones used for the general thermal field equation (section 3.6) for consistency. As F denotes the product of the electric field and the elementary charge, then it was decided that F_e will be used for the electric field.

whose zero is on the metal boundary and the positive direction is away from the metal. q is the elementary charge and ϵ_0 is the electric constant.

Electron field emission current density J_{F0} is characterised by the Fowler-Nordheim equation

$$J_{F0}(F_e,\Phi) = \frac{aF_e^2}{\Phi\tau(F_e)^2}\exp\left(-\nu(F_e)\frac{b\Phi^{\frac{3}{2}}}{F_e}\right), \tag{2.3}$$

where $a = \frac{q^3}{8\pi h_P}$ and $b = \frac{8\pi\sqrt{2m}}{3eh_P}$ are the Fowler-Nordheim first and the second constant, respectively; τ and ν are correction factors, that depend on the shape of the metal surface energy barrier. For the Schottky-Nordheim barrier (2.2) [6]

$$\nu(F_e) \approx 1 - \frac{F_e}{F_b} + \frac{1}{6}\frac{F_e}{F_b}\ln\frac{F_e}{F_b} \tag{2.4}$$

and

$$\tau(F_e) \approx 1 + \frac{F_e}{9F_b}\left(1 - \frac{1}{2}\ln\frac{F_e}{F_b}\right), \tag{2.5}$$

where F_b is the critical electric field, which reduces the energy barrier with height Φ to zero. In the case of Schottky-Nordheim barrier

$$F_b = \frac{4\pi\epsilon_0\Phi^2}{q^3}. \tag{2.6}$$

The equation 2.3 is known as the standard Fowler-Nordheim equation, which has been derived strictly for absolute zero temperature. In the case of non-zero temperature T, it must be multiplied by a temperature correction factor

$$J_F(F_e,T) = \Theta(F_e,T)J_{F0}(F_e). \tag{2.7}$$

The factor $\Theta(F_e,T)$ is given by [5]

$$\Theta(F_e,T) = \frac{\pi k_B T/d_T}{\sin(\pi k_B T/d_T)}, \tag{2.8}$$

where $d_T = \frac{2F_e}{3b\sqrt{\Phi}}$ is a parameter, which describes the lowering of the energy barrier.

2.3 Applicability regions emission equations

Thermionic and field emission have non-overlapping applicability regions [7]. Under high temperature and relatively low field conditions, the emission current is characterised by the Richardson's equation (2.1), and in low temperature and high field conditions, the current is characterised by Fowler-Nordheim equation (2.3) (for copper see figure 2.1). Between the thermionic and field emission regions, there is the so-called transition or intermediate region,

where neither of the two equations describe the current accurately.

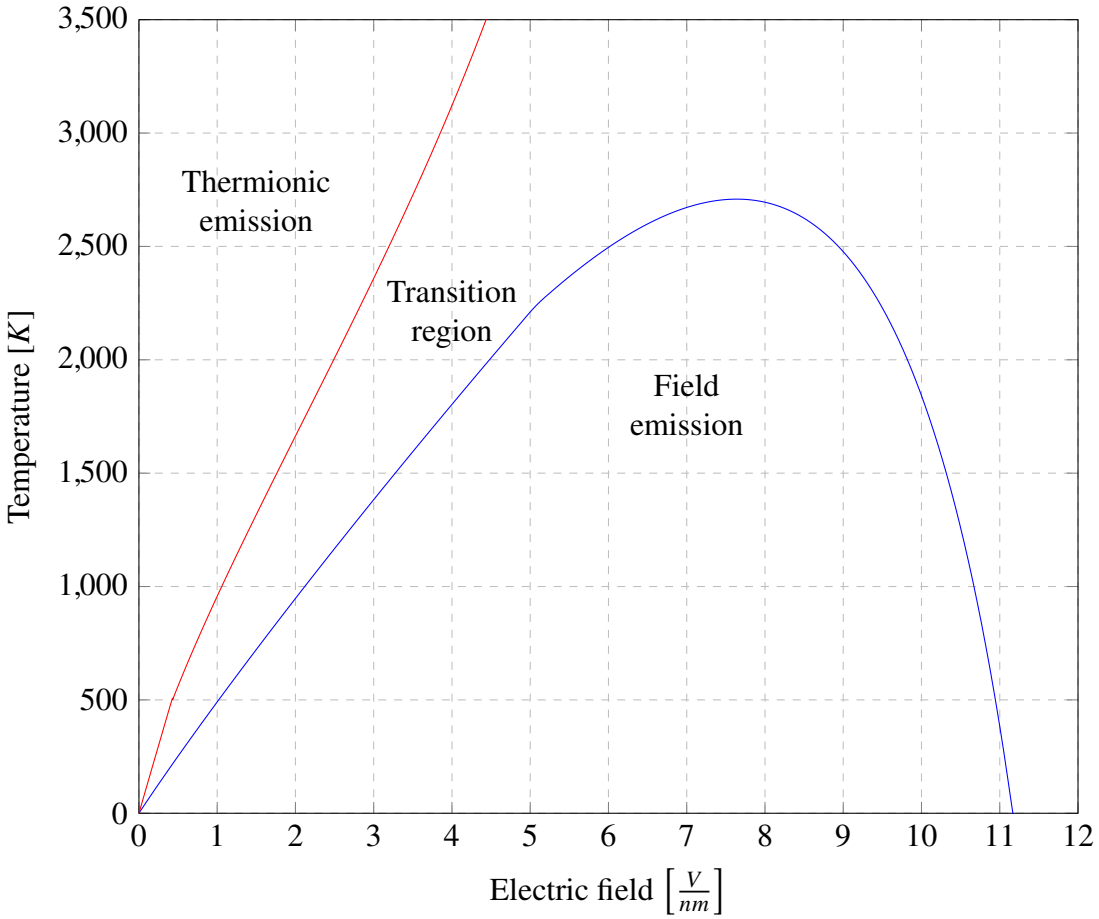

Figure 2.1: Applicability regions for Richardson's and Fowler-Nordheim equations for copper (work function $\Phi = 4.5eV$). Region are based on [7].

3. Methodology

3.1 Simulated system

The simulated system consists of a single copper protrusion on the surface of an otherwise smooth copper cathode. The dimensions will be varied throughout the work, but the protrusion's dimensions will be in the order of 10 nanometers and the simulation box needs to be large enough to disregard boundary effects. The shape of the protrusion will also be varied.

The system is three dimensional and is symmetric about its central vertical axis. A cross section through the symmetrical axis can be seen in figure 3.1.

Three boundary value problems need to be solved. The first one is finding the electric field in the vacuum (section 3.2), the second is finding the electrical currents in copper (section 3.3) due to electron emission (see sections 2.1, 2.2 and 3.6). The third boundary value problem is finding the temperature distribution in the copper (see section 3.4).

Should the following be in this section?

The electric potential in the vacuum and in the copper will be handled independently. Potential in the vacuum will be denoted as φ_v and in the copper will be φ_c. This treatment is not strictly correct, as the potentials should match on the copper-vacuum boundary, but the effect is small and thus is ignored in this work. Is this reasonable? Small changes in electric field SHOULD cause huge changes in current (exponential dependence in emission equations).

All equations are stationary. Because electrical and thermal processes are much faster than the experimental time scale (seconds).

3.2 Electric field

Also mention Laplace's equation.

In the simulated system (see figure 3.1), the electric field configuration corresponding to the boundary conditions needs to be found in the vacuum.

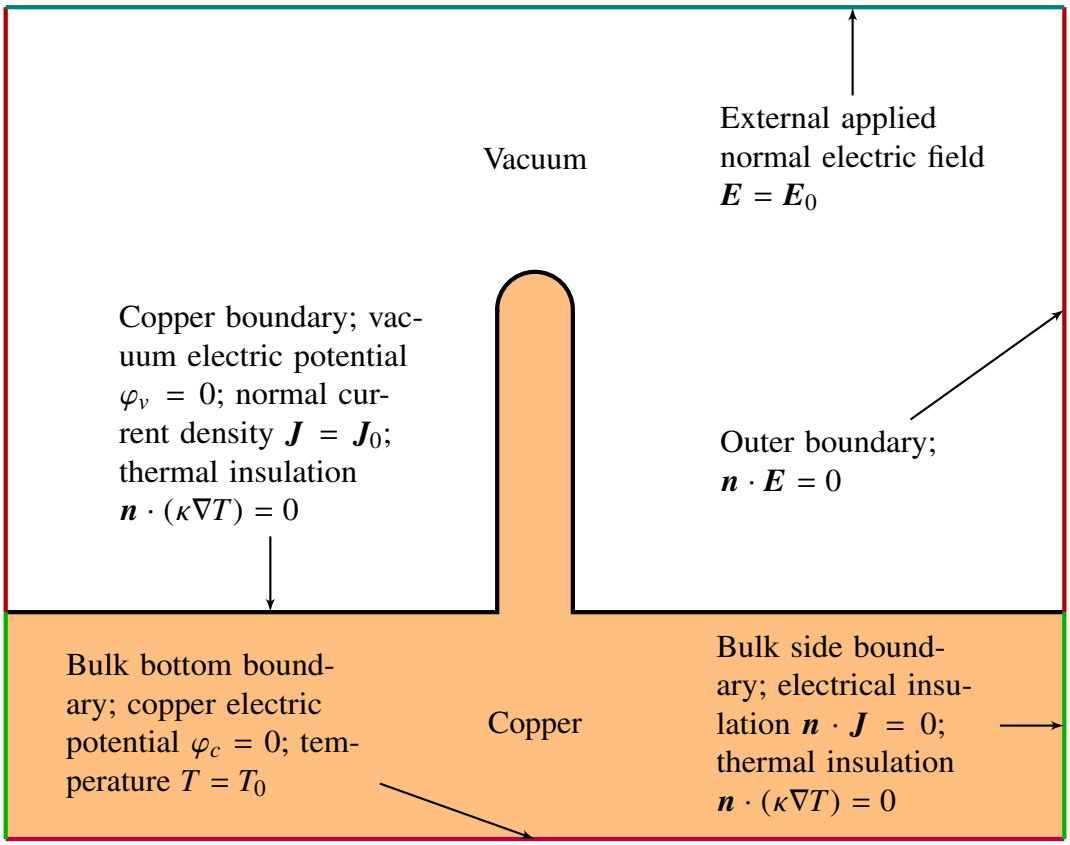

Figure 3.1: Simulated system, boundary conditions (descriptions of boundary conditions are in the corresponding sections).

3.2.1 Poisson's equation

The electric potential (and field) configuration in a system can be found by solving the *Poisson's equation*

$$\nabla^2 \varphi(\boldsymbol{r}) = -\frac{\rho(\boldsymbol{r})}{\epsilon_0}, \tag{3.1}$$

where $\varphi(\boldsymbol{r})$ is the electrostatic potential, $\rho(\boldsymbol{r})$ is the space charge density and ϵ_0 is the electric constant.

3.2.2 Boundary conditions without headings

The Poisson's equation 3.1 has three different boundary conditions (see figure 3.1). The top side of the simulation box has a Neumann boundary condition corresponding to the applied external electric field $\boldsymbol{E}_0$

$$-\nabla \varphi_v(\boldsymbol{r}) = \boldsymbol{E}(\boldsymbol{r}) = \boldsymbol{E}_0, \tag{3.2}$$

where $\varphi_v(\boldsymbol{r})$ is the potential in the vacuum[1] and $\boldsymbol{E}(\boldsymbol{r})$ is the electric field. The sides of the simulation box (vacuum boundary) have also a Neumann boundary condition

$$\boldsymbol{n} \cdot (-\nabla\varphi_v(\boldsymbol{r})) = \boldsymbol{n} \cdot \boldsymbol{E}(\boldsymbol{r}) = 0, \tag{3.3}$$

where $\boldsymbol{n}$ is the surface normal vector. This corresponds to a periodic boundary condition and if the simulation box is large enough, the periodicity does not affect the field configuration near the protrusion.

The copper-vacuum boundary has a Dirichlet boundary condition

$$\varphi_v(\boldsymbol{r}) = 0, \tag{3.4}$$

due to copper, as a conductive metal, having a constant potential over its surface. This statement isn't strictly true, because the copper has currents (due to electron emission) flowing through it, but considering that the potential difference due to currents is multiple orders of magnitude smaller than the potential difference due to the external applied electric field, the effect is ignored. Should I prove this? Is it really so? Small changes in electric field SHOULD cause huge changes in current (exponential dependence in emission equations).

3.2.3 Field enhancement?

3.2.4 Space-charge screening?

3.3 Electric currents

Should conductance and nanoscale effects be put in this section?? Probably...

The electric currents will be found in the copper part of the system (see figure 3.1). The stationary differential equation for finding the potential corresponding to currents can be derived by combining the continuity equation with the differential Ohm's law and it can be represented as

$$\nabla \cdot (\sigma\nabla\varphi) = 0, \tag{3.5}$$

where σ is the conductivity and φ is the electric potential. And the current density $\boldsymbol{J}$ can be found by the differential Ohm's law

$$\boldsymbol{J} = \sigma\boldsymbol{E} = \sigma\nabla\varphi. \tag{3.6}$$

[1]The difference between vacuum and copper potential must be denoted, as the boundary conditions do not match. See section 3.1.

3.3.1 Boundary conditions

The equation 3.5 has three different boundary conditions in the system (see figure 3.1). The first one is a Neumann boundary condition that corresponds to the electron emission current

$$\boldsymbol{J} = \sigma \nabla \varphi_c = \boldsymbol{J}_0(\boldsymbol{E}, T), \tag{3.7}$$

where $\boldsymbol{J}$ is the current density, φ_c is the electric potential in copper[2] and $\boldsymbol{J}_0(\boldsymbol{E}, T)$ is the emission current, which is generally dependent on the local electric field $\boldsymbol{E}$ and the temperature T (see sections 2.1, 2.2 and 3.6).

The bulk sides have a Neumann boundary condition corresponding to thermal insulation

$$\boldsymbol{n} \cdot \boldsymbol{J} = \boldsymbol{n} \cdot (\sigma \nabla \varphi_c) = 0, \tag{3.8}$$

where $\boldsymbol{n}$ is the surface normal vector of the boundary.

The bottom of the bulk has a Dirichlet boundary condition corresponding to a constant electric potential

$$\varphi_c = 0. \tag{3.9}$$

3.4 Heating

3.4.1 Heat equation

In nanoscale systems, thermal processes are very fast (How fast?) compared to the experimental time scale in our case (seconds). Therefore, the temperature distribution can be found using the stationary (i.e. steady state) heat equation

$$\nabla \cdot (\kappa(T) \nabla T) = \rho(T) J(T)^2, \tag{3.10}$$

where κ is the thermal conductivity, T is the temperature, ρ is the resistivity and J is the current density. The right side of equation 3.10 represents the volumetric resistive heating.

The radiative cooling has been ignored as ... (Citation to Stefan's article?)

3.4.2 Boundary conditions

In the system, the heat equation (3.10) has two different boundary conditions (see figure 3.1). The copper boundary and the copper bulk side boundary have the Neumann boundary condition corresponding to thermal insulation

$$\boldsymbol{n} \cdot (\kappa \nabla T) = 0, \tag{3.11}$$

[2]Distiction must be made from vacuum potential, as the boundary conditions do not match, see section 3.1.

where $\boldsymbol{n}$ is the surface normal vector. The bulk bottom boundary has the Dirichlet condition

$$T = T_0, \tag{3.12}$$

where T_0 is the temperature of outer environment (usually $T_0 = 293.15K$).

3.4.3 Electrical conductivity

The temperature dependence of the resistivity of copper $\rho(T)$ (and thus the electrical conductivity $\sigma(T) = \frac{1}{\rho(T)}$) can be accurately described by an equation developed by Matula [8] and improved by Schuster et al. [9], which is of the form

$$\rho(T) = A\left[1 + \frac{BT}{\theta - CT} + D\left(\frac{\theta - CT}{T}\right)^p\right]\Phi\left(\frac{\theta - CT}{T}\right) + \rho_0, \tag{3.13}$$

where θ, A, B, C, D, p, ρ_R are constants and

$$\Phi(x) = \frac{4}{x^5}\int_0^x \frac{z^5 e^z}{(e^z - 1)^2} dz. \tag{3.14}$$

The values of the constants can be found by fitting equation 3.13 to experimental data. According to Schuster et al. [9], the best fit is achieved with the following values[3]

$$\begin{aligned} A &= 1.816013 \times 10^{-8}\Omega m, \\ B &= -2.404851 \times 10^{-3}, \\ C &= 4.560643 \times 10^{-2}, \\ D &= -5.976831 \times 10^{-3}, \\ p &= -1.838419, \\ \theta &= 310.8K, \\ \rho_R &= 1.803751 \times 10^{-12}\Omega m. \end{aligned} \tag{3.15}$$

The equation 3.13 is applicable from 20 K to 1357.6 K (i.e. until the melting point).

Schuster et al. also found a small correction factor to the resistivity due to thermal expansion [9], but the model of the current work does not consider thermal expansion and thus the correction factor can be ignored.

In computer simulations, calculate points and use logarithmic (?) interpolation (stefan2009)

[3] Some of the values in article [9] are incorrect, the correct values can be found in the appendix of the same article.

3.4.4 Thermal conductivity

The thermal conductivity of a material depends on two effects: the lattice thermal conduction, caused by interatomic interactions and the electronic thermal conduction, caused by electronic effects. In copper (and most metals), the lattice thermal conduction is negligible compared to the electronic thermal conduction [10], and thus it is ignored in this work. The electronic component of the thermal conductivity can be calculated by the Wiedemann-Franz law [11]

$$\kappa(T) = LT\sigma(T), \tag{3.16}$$

where T is the temperature, $\sigma(T)$ is the electrical conductivity (found by 3.13) and $L = 2.443 \times 10^{-8} W\Omega K^{-2}$ is the Lorenz number.

The Wiedemann-Franz law is known to not be applicable under certain intermediate temperature conditions. The law has found to be valid for copper films above the temperature of 200 K [12]. The system in this work is studied above 200 K and thus the law is applicable throughout this work.

3.4.5 Nanoscale size effects (to Section heading)

In a large enough bulk material, the mean free path of electrons is mainly determined by electron-phonon and electron-defect scattering, as electron-electron and electron-boundary scattering are negligible. When the characteristic length, such as the diameter of the protrusion on copper surface or the size of grains (for a polycrystalline solid), is comparable with the bulk mean free path of electrons, boundary scattering becomes important. Subsequently, the electrical conductivity σ and the thermal conductivity κ become size dependent. [13, pp. 174-182]

The size dependence is usually characterized by the Knudsen number $Kn = \lambda_b/d$, where λ_b is the bulk mean free path of electrons and d is the characteristic length (e.g. the diameter of a protrusion). The size dependent electrical and thermal conductivities can be expressed as

$$\begin{aligned} \sigma_{nano} &= F(Kn) \cdot \sigma_b, \\ \kappa_{nano} &= F(Kn) \cdot \kappa_b, \end{aligned} \tag{3.17}$$

where σ_b and κ_b are the bulk conductivities. The finite size effects correction factor $F(Kn)$ for a thin cylindrical wire can be found using [13, p. 182]

$$\begin{aligned} F(Kn) &= 1 - \frac{12(1-p)^2}{\pi} \sum_{m=1}^{\infty} m p^{m-1} G(Kn, m), \\ G(Kn, m) &= \int_0^1 \sqrt{1-\xi^2} \int_1^{\infty} \exp\left(-\frac{m\xi t}{Kn}\right) \frac{\sqrt{t^2-1}}{t^4} dt d\xi, \end{aligned} \tag{3.18}$$

where p is the specularity, which is defined as the probability that a boundary scattering event is elastic and specular and it depends on the surface roughness.

Asymptotic approximations for 3.18 are [14]

$$\text{for } Kn \ll 1: \quad F(Kn) \approx 1 - \frac{3Kn}{4}(1-p) + \frac{3Kn^3}{8}(1-p)^2 \sum_{v=1}^{\infty} \frac{p^{v-1}}{v^2}, \tag{3.19}$$

$$\text{for } Kn \gg 1: \quad F(Kn) \approx \frac{1+p}{1-p}\frac{1}{Kn} - \frac{3}{8Kn^2}\left[\frac{1+4p+p^2}{(1-p)^2}(\ln(Kn)+1.059) - (1-p)^2 \sum_{v=1}^{\infty}(v^3 p^{v-1} \ln v)\right] - \frac{2}{15Kn^3}\frac{(1+11p+11p^2+p^3)}{(1-p)^3}. \tag{3.20}$$

The factor $F(Kn)$ can also be calculated using a simulation program by Yarimbiyik et al. [15, 16]. The simulation program calculates the effective conductances for thin film and line interconnections with a rectangular cross-sectional surface area and takes the dimensions of the system, grain structure and specularity as input.

The specularity value p for copper has been taken to be 0.01 in this work, which is close to the values reported in literature [17–19]. citation range (i.e. [17-19]).

The Lorenz number L from the Wiedemann-Franz law (equation 3.16) also has a finite size dependence [20], due to phonon conductivity of copper becoming more important as the finite size decreases. This effect is very small and thus is ignored in this work.

λ_b **and thus** Kn **and also the finite size effects depend on temperature!** (Similar derivation in [15]) (Is the denotation non-conflicting with the remaining work?)

According to the Drude model of electrical conduction, the conductivity σ can be expressed as

$$\sigma = \frac{nq^2\tau}{m}, \tag{3.21}$$

where n, q, m and τ are respectively an electron's number density, charge, effective I THINK NOT? mass and average relaxation time. τ can be related to the mean free path by $\tau = \lambda_b / v_F$, where v_F is the Fermi velocity. Thus, σ can be expressed as

$$\sigma(T) = \frac{nq^2\lambda_b(T)}{mv_F}. \tag{3.22}$$

By assuming that n, q, m, v_F are constant with temperature, the dependence of λ_b on temperature can be found. The mean free pa citeth of electrons λ_b for copper at room temperature (298 K) is ... [citation]. Thus,

$$\lambda_b(T) = \frac{\lambda_b(298\,\mathrm{K})}{\sigma(298\,\mathrm{K})}\sigma(T). \tag{3.23}$$

3.5 Work function dependence on size?

Assume a constant work function... it might depend on ... but can be ignored as ... [some citations] Move this under "Simulated system"?

3.6 General thermal field emission

What energy barrier at the surface? Schottky-Nordheim (same as FN).

Regions of validity?

Reference the private communications with Jensen.

The emission current in the transition region can be found by numerical integration, but that is not suitable for computational simulations. Jensen et al. have developed an analytical equation, the general thermal field emission equation, which describes the emission current in the transition region and also in the thermionic and field regions [21, 22]. It is expressed as

$$\begin{aligned} J_{GTF}(F,T) &= A_{RLD}T^2 N\left(\frac{\beta_T}{\beta_F(E_m)}, \beta_F(E_m)(E_o-\mu)\right), \\ N(n,s) &\approx n^2\Sigma\left(\frac{1}{n}\right)e^{-s} + \Sigma(n)e^{-ns}, \end{aligned} \tag{3.24}$$

where J_{GTF} is the current density, F is the product of local electric field and elementary charge, T is temperature, A_{RLD} is the Richardson's constant (see equation 2.1), $\beta_T = \frac{1}{k_B T}$ is the thermal emission energy slope factor, $\beta_F(E_m)$ field emission energy slope factor, E_o is an energy parameter, μ is the chemical potential (fermi level) and $\Sigma(x)$ is a function characteristic to the equation. $\Sigma(x)$ has been approximated in [21, p. 7] with the equation:

$$\Sigma(x) \approx \frac{1}{1-x} - x(1+x) + \frac{1}{4}x^3(7x-3) + \zeta(2)x^2(1-x^2), \tag{3.25}$$

where $\zeta(x)$ is the Riemann zeta function. $\Sigma(n)$ experiences a discontinuity at $n = 1$ but the function $N(n,s)$ (from equation 3.24) remains finite, as

$$\lim_{n\to 1} N(n,s) = e^{-s}(1+s). \tag{3.26}$$

β_F can be calculated with the equation (43) in reference [21]

$$\beta_F(E) \approx \frac{1}{\phi}[B_q z + C_{FN}(1-z) + 3(2B_{FN} - B_q - C_{FN})z(1-z)], \tag{3.27}$$

where the expressions of relevant parameters are in table 3.1 and used constants are in table 3.2.

In the general thermal field equation 3.24, $\beta_F(E)$ is always evaluated at E_m. E_m is an energy

Parameter	Description	Equation or page in [21]
$z = \frac{E-\mu}{\phi}$	-	p. 6
$B_q = C_q = \frac{\pi}{\hbar}\phi\sqrt{2m}\left(\frac{Q}{F^3}\right)^{1/4}$	-	(41)
$B_{FN} = \frac{4}{3\hbar F}\sqrt{2m\Phi^3}\nu(y)$	Fowler-Nordheim's B constant	(40)
$C_{FN} = \frac{2\phi}{\hbar F}\sqrt{2m\Phi}t(y)$ [a]	Fowler-Nordheim's C constant	(40)
$Q = \frac{q^2}{16\pi\epsilon_0}$	image potential factor	p. 6
$\phi = \Phi - \sqrt{4QF}$	potential barrier lowering	p. 6
$y = \frac{\sqrt{4QF}}{\Phi}$	barrier lowering parameter	p. 6
$\nu(y) \approx (1-y^2) + \frac{1}{3}y^2 ln(y)$	elliptical integral term (Forbes approx.)	(21)
$t(y) \approx \frac{1}{9}y^2(1-ln(y)) + 1$	elliptical integral term (Forbes approx.)	(23)
$\beta_T = \frac{1}{k_B T}$	thermal emission energy slope factor	-

Table 3.1: Expressions and descriptions for parameters used in the general thermal field equation. All of them are taken from reference [21].

[a] There was an error in [21], see [23, p. 46] equation (30).

parameter, which depends on the emission regime (see table I in [21]) and can be found by

$$E_m = \mu + \phi, \qquad \text{when } T > T_{max} \tag{3.28}$$

$$\beta_F(E_m) = \beta_T, \qquad \text{when } T_{min} \leq T \leq T_{max} \tag{3.29}$$

$$E_m = \mu, \qquad \text{when } T < T_{min}, \tag{3.30}$$

where

$$T_{min} = \frac{1}{k_B \beta_F(\mu)} \tag{3.31}$$

$$T_{max} = \frac{1}{k_B \beta_F(\mu+\phi)}. \tag{3.32}$$

The equation 3.29 is a quadratic equation, whose greater[4] root is the correct E_m. Using equation 3.27, we get

$$[-3(2B_{FN} - B_q - C_{FN})]z_m^2 + [3(2B_{FN} - B_q - C_{FN}) + B_q - C_{FN}]z_m + [C_{FN} - \phi B_T] = 0. \tag{3.33}$$

[4] Reference [21, p. 7] states that the smaller root is the correct one, but the author of this work achieved matching results with [22] by using the greater root.

Constant	Description	Value
Φ	work function	$4.5eV$
μ	chemical potential (Fermi level)	$7eV$
q	elementary charge	$1.602\,176\,57 \times 10^{-19}C$
ϵ_0	electric constant	$1.418\,597\,23 \times 10^{-39}\frac{C^2}{eVnm}$
A_{RLD}	Richardson's constant	$120.17349\frac{A}{K^2cm^2}$
k_B	Boltzmann's constant	$\frac{1}{11604.506}\frac{eV}{K}$
m	mass of electron	$\frac{510998.9}{(2.997\,924\,58 \times 10^{17})^2}\frac{eV}{(nm/s)^2}$
$\hbar$	Planck's reduced constant	$6.582\,119\,28 \times 10^{-16}eVs$

Table 3.2: Relevant constants and their values.

Solving it for the z_m that corresponds to the greater root of E_m, we get

$$\begin{aligned} z_m &= \frac{-b}{2a} + \sqrt{\left(\frac{b}{2a}\right)^2 - \frac{c}{a}}, \\ a &= -3(2B_{FN} - B_q - C_{FN}), \\ b &= 6B_{FN} - 2B_q - 4C_{FN}, \\ c &= C_{FN} - \phi B_T. \end{aligned} \tag{3.34}$$

The ratio of energy slope factors $n = \frac{\beta_T}{\beta_F(E_m)}$ and the parameter $s = \beta_F(E_m)(E_o - \mu)$ can now be calculated by the following relations (see table I in [21]):

$$n = \begin{cases} \frac{\beta_T \phi}{B_q} & \text{when } T > T_{max} \\ 1.0 & \text{when } T_{min} \leq T \leq T_{max} \\ \frac{\beta_T \phi}{C_{FN}} & \text{when } T < T_{min}, \end{cases} \tag{3.35}$$

$$s = \begin{cases} B_q & \text{when } T > T_{max} \\ B_{FN} + \frac{b}{2}z_m^2 + \frac{2a}{3}z_m^3 & \text{when } T_{min} \leq T \leq T_{max} \\ B_{FN} & \text{when } T < T_{min}, \end{cases} \tag{3.36}$$

Using the previous two relations (3.35 and 3.36), the general thermal field equation 3.24 can be evaluated.

A concise summary of this implementation as a flowchart can be seen in figure 3.2. Also an implementation of this with the COMSOL Multiphysics simulation software package can be found in appendix A.

3.7 Finite element method

COMSOL manual/documentation

Solution to last time step is initial condition to next time step.

The finite element method (FEM) [24–28] is a numerical technique used to solve boundary value problems for differential equations. The method is used by first constructing a geometric model of the system and dividing it into non-overlapping simple shaped subdomains or *elements* (which consitute the *mesh*). Each element has a number of nodes, which parameter (?) values are used to approximate the values in every other point of the element by using polynomials. The differential equations can be used to find element-wide (algebraic or OD) equations for the node values. Using all the element equations and the boundary and initial conditions, the system of equations for the whole model can be found. For steady-state problems, this will be a system of algebraic equations, and for a transient problem, it will be a system of ODE's. The first case is usually solved by (gaussian elimination, cholesky, NOPE-> Pardiso, MUMPS) and the second case can be solved by implicit or explicit methods?! !VERY ROUGH DRAFT!

In this work, the finite element method is used to solve the Poisson's equation for the electric field (equation 3.1), the equation for electric currents (equation 3.5) and the heat equation (equation 3.10).

3.7.1 Mesh

Mesh convergence figure...?

3.7.2 Initial conditions should this be here?

3.7.3 Solver algorithms

3.7.4 Newton's method

3.7.5 Pardiso/mumps

3.7.6 Scaling electric field

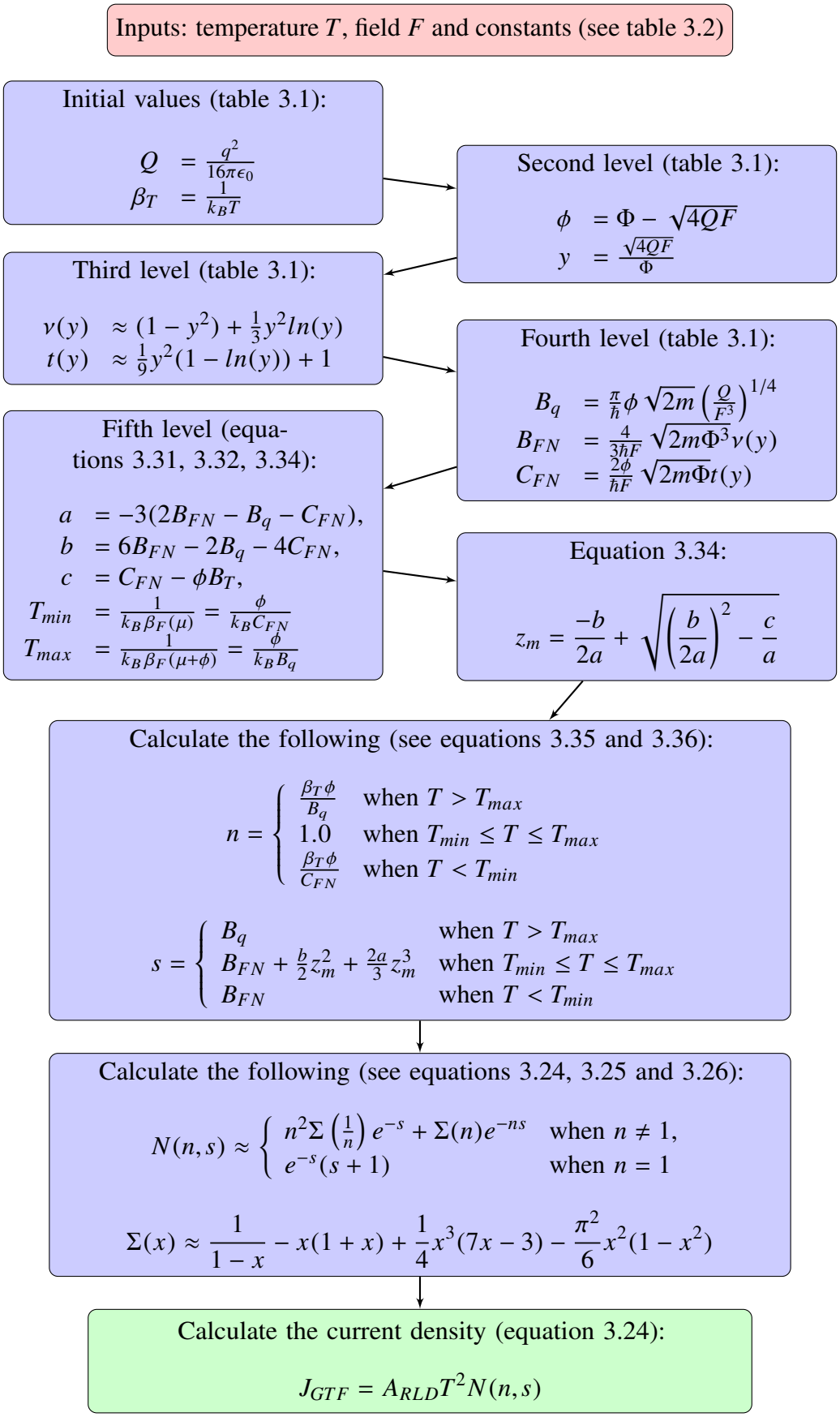

Figure 3.2: Implementation flowchart. Parameters are placed in a node, when all of their dependencies are already calculated in previous nodes.

4. Results

5. Summary/Conclusion

References

[1] *Compact Linear Collider*. 2013. URL: http://clic-study.org/.

[2] *Multiphysics Modeling and Simulation Software - COMSOL*. 2013. URL: http://www.comsol.com/.

[3] M E Kiziroglou et al. "Thermionic field emission at electrodeposited Ni–Si Schottky barriers". In: *Solid-State Electronics* 52.7 (2008), pp. 1032–1038.

[4] Jon Orloff. *Handbook of Charged Particle Optics*. CRC Pr Llc, 2008, pp. 5–6.

[5] Richard G Forbes. "Use of energy-space diagrams in free-electron models of field electron emission". In: *Surface and interface analysis* 36.5-6 (2004), pp. 395–401.

[6] Richard G Forbes. "Simple good approximations for the special elliptic functions in standard Fowler-Nordheim tunneling theory for a Schottky-Nordheim barrier". In: *Applied physics letters* 89.11 (2006), p. 113122.

[7] E L Murphy and R H Good. "Thermionic Emission, Field Emission, and the Transition Region". In: *Phys. Rev.* 102.6 (June 1956), pp. 1464–1473. DOI: 10.1103/PhysRev.102.1464. URL: http://link.aps.org/doi/10.1103/PhysRev.102.1464.

[8] Richard Allen Matula. "Electrical resistivity of copper, gold, palladium, and silver". In: *Journal of Physical and Chemical Reference Data* 8 (1979), p. 1147.

[9] Constance E Schuster, Mark G Vangel, and HA Schafft. "Improved estimation of the resistivity of pure copper and electrical determination of thin copper film dimensions". In: *Microelectronics Reliability* 41.2 (2001), pp. 239–252.

[10] Bo Feng, Zhixin Li, and Xing Zhang. *Role of phonon in the thermal and electrical transports in metallic nanofilms*. May 2009. DOI: 10.1063/1.3129707. URL: http://scitation.aip.org/content/aip/journal/jap/105/10/10.1063/1.3129707.

[11] Roger J. Elliott and Alan F. Gibson. *An Introduction to Solid State Physics and Its Applications*. Macmillan, 1974, p. 490. ISBN: 0333110234. URL: http://books.google.com/books?id=DugNAQAAIAAJ&pgis=1.

[12] Prem Nath and K.L. Chopra. "Thermal conductivity of copper films". In: *Thin Solid Films* 20.1 (Jan. 1974), pp. 53–62. ISSN: 00406090. DOI: 10.1016/0040-6090(74)90033-9. URL: http://www.sciencedirect.com/science/article/pii/0040609074900339.

[13] Zhuomin Zhang. *Nano/Microscale Heat Transfer*. McGraw Hill Professional, 2007, p. 479. ISBN: 0071509739. URL: http://books.google.ee/books/about/Nano_Microscale_Heat_Transfer.html?id=64ygtm0HWtcC&pgis=1.

[14] R. B. Dingle. "The Electrical Conductivity of Thin Wires". In: *Proceedings of the Royal Society A: Mathematical, Physical and Engineering Sciences* 201.1067 (May 1950), pp. 545–560. ISSN: 1364-5021. DOI: 10.1098/rspa.1950.0077. URL: http://rspa.royalsocietypublishing.org/content/201/1067/545.short.

[15] AE Yarimbiyik et al. "Modeling and simulation of resistivity of nanometer scale copper". In: *Microelectronics Reliability* 46.7 (July 2006), pp. 1050–1057. ISSN: 00262714. DOI: 10.1016/j.microrel.2005.09.004. URL: http://linkinghub.elsevier.com/retrieve/pii/S0026271405003173.

[16] AE Yarimbiyik, ME Zaghloul, and HA Schafft. *Implementation of simulation program for modeling the effective resistivity of nanometer scale film and line interconnects*. 2006. URL: http://nvl.nist.gov/pub/nistpubs/ir/2006/ir7234.pdf.

[17] AE Yarimbiyik et al. "Experimental and simulation studies of resistivity in nanoscale copper films". In: *Microelectronics Reliability* 49.2 (Feb. 2009), pp. 127–134. ISSN: 00262714. DOI: 10.1016/j.microrel.2008.11.003. URL: http://www.sciencedirect.com/science/article/pii/S0026271408004058.

[18] E. H. Sondheimer. "The mean free path of electrons in metals". In: *Advances in Physics* 50.6 (Sept. 2001), pp. 499–537. ISSN: 0001-8732. DOI: 10.1080/00018730110102187. URL: http://www.tandfonline.com/doi/abs/10.1080/00018730110102187.

[19] H. H. Mende and G. Thummes. "Surface scattering of electrons on copper whiskers and its influence on the electrical resistivity at 4.2 K". In: *Applied Physics* 6.1 (Feb. 1975), pp. 93–97. ISSN: 0340-3793. DOI: 10.1007/BF00883555. URL: http://link.springer.com/10.1007/BF00883555.

[20] D. Jou, V.A. Cimmelli, and A. Sellitto. "Nonlocal heat transport with phonons and electrons: Application to metallic nanowires". In: *International Journal of Heat and Mass Transfer* 55.9-10 (Apr. 2012), pp. 2338–2344. ISSN: 00179310. DOI: 10.1016/j.ijheatmasstransfer.2012.01.033. URL: http://www.sciencedirect.com/science/article/pii/S0017931012000452.

[21] K L Jensen. "General formulation of thermal, field, and photoinduced electron emission". In: *Journal of Applied Physics* 102.2 (2007), p. 24911. ISSN: 00218979. DOI: 10.1063/1.2752122. URL: http://scitation.aip.org/content/aip/journal/jap/102/2/10.1063/1.2752122.

[22] K L Jensen et al. "Electron emission contributions to dark current and its relation to microscopic field enhancement and heating in accelerator structures". In: *Physical Review Special Topics-Accelerators and Beams* 11.8 (2008), p. 81001.

[23] W Zhu. *Vacuum microelectronics*. Wiley, 2001. ISBN: 9780471322443. URL: http://books.google.ee/books?id=iShTAAAAMAAJ.

[24] Olek C Zienkiewicz, Robert L Taylor, and J.Z. Zhu. *The Finite Element Method: Its Basis and Fundamentals*. Butterworth-Heinemann, 2005, p. 752. ISBN: 008047277X. URL: http://books.google.ee/books/about/The_Finite_Element_Method_Its_Basis_and.html?id=YocoaH8lnx8C&pgis=1.

[25] Christian Grossmann and Hans-Görg Roos. *Numerical Treatment of Partial Differential Equations*. Springer Science and Business Media, 2007, p. 591. ISBN: 3540715827. URL: http://books.google.com/books?id=lmtboXIXttAC&pgis=1.

[26] G.R. Liu and S. S. Quek. *The Finite Element Method: A Practical Course*. Elsevier Science, 2013, p. 464. ISBN: 0080994415. URL: http://books.google.com/books?id=ZYEKAQAAQBAJ&pgis=1.

[27] Pei-bai Zhou. *Numerical Analysis of Electromagnetic Fields*. Springer Berlin Heidelberg, 2012, p. 406. ISBN: 3642503217. URL: http://books.google.com/books?id=QwmSngEACAAJ&pgis=1.

[28] Singiresu S. RAO. *The Finite Element Method in Engineering*. Butterworth-Heinemann, 2011, p. 688. ISBN: 0080470505. URL: http://books.google.com/books?id=7n6k2NmGU48C&pgis=1.

A. COMSOL implementation

The COMSOL implementation of the general thermal field equation is presented here. It consists of three COMSOL variable groups. First one contains all relevant constants (table A.1), the second one contains the main equations (table A.3) and the third one contains smoothed variables (table A.4). The sigma function (described in equation 3.25) is implemented as a COMSOL function, see table A.2.

As COMSOL is not able to perform some arithmetic operations on values with units, then all the variables need to be unitless. The unit system used will be the same as in [22] and can be inspected by studying the table A.1.

A.1 Constants

Name	Expression	Description
e_charge	1.60217657e-19	elementary charge, C
eps_0	1.41859723e-39	electric constant, C^2/(eV*nm)
k_B	1/11604.506	Boltzmann's constant, eV/K
me	510998.9/((2.99792458*10^(17))^2)	mass of electron, eV/(nm/s)^2
h_bar	6.58211928e-16	Planck's reduced constant, eV*s
h_p	h_bar*2*pi	Planck's constant, eV*s
A_RLD	120.17349	Richardson's constant, A/(K^2* cm^2)
cu_Phi	4.5	work function of copper, eV
cu_mu	7	chemical potential/fermi level of copper, eV

Table A.1: COMSOL implementation: constants.

A.2 Functions

Function name:	GTFE_sigma
Expression:	1/(1-x)-(x*(1+x)-1/4*x^3*(7*x-3)-pi^2/6*x^2*(1-x^2))
Arguments:	x

Table A.2: COMSOL implementation: functions.

A.3 Main equations

As the variables need to be unitless, the input values, such as the temperature T and field F (which are supplied by COMSOL and come with units) need to be multiplied by their inverted units.

Name	Expression	Description
g_T	T[1/K]	Temperature (K)
g_normE	-V_lm/(epsilon0_const*2*pi*r)* 1[F]*1[V/m]	local electric field (V/m); includes Comsol-specific variables; more accurate than es.normE
g_F	max(g_normE*1[m/V]*1e-9,1e-12)	product of local electric field strength and elementary charge (eV/nm)
g_Q	e_charge^2/(16*pi*eps_0)	Image potential factor
g_phi	max(cu_Phi-(4*g_Q*g_F)^(1/2),0.2)	barrier lowering
g_y	(4*g_Q*g_F)^(1/2)/cu_Phi	parameter, which depends on barrier lowering
g_beta_T	1/(k_B*g_T)	slope factor of thermal emission
g_B_q	(pi/h_bar*g_phi)*sqrt(2*me)* (g_Q/g_F^3)^(1/4)	Quadratic representation parameter
g_nu	(1-g_y^2)+1/3*g_y^2*log(g_y)	FN's nu (elliptical integral function)
g_t	1/9*g_y^2*(1-log(g_y))+1	FN's tau (elliptical integral function)
g_B_FN	(4/(3*h_bar*g_F))*sqrt(2*me* cu_Phi^3)*g_nu	FN's B
g_C_FN	(2*g_phi/(h_bar*g_F))*sqrt(2*me* cu_Phi)*g_t	FN's C
g_T_min	1/(k_B*1/g_phi*(g_C_FN))	Under this is field emission region
g_T_max	1/(k_B*1/g_phi*(g_B_q))	Over this is thermionic emission region
g_a	-3*(2*(g_B_FN)-g_B_q-(g_C_FN))	Variable for finding E_m I

g_b	3*(2*(g_B_FN)-g_B_q-(g_C_FN))+ g_B_q-(g_C_FN)	Var II
g_c	(g_C_FN)-g_phi*g_beta_T	Var III
g_z	-g_b/(2*g_a)+sqrt((g_b/(2*g_a))^2-g_c/g_a)	z value (corresponding to E_m) in transition region
g_s	if(g_T>g_T_max,g_B_q, if(g_T<g_T_min,g_B_FN,g_B_FN+(g_b/2)*g_z^2+2/3*g_a*g_z^3))	-
g_n	if(g_T>g_T_max, g_beta_T/(g_B_q/g_phi), if(g_T<g_T_min, g_beta_T/(g_C_FN/g_phi),1.0))	Ratio of energy slope factors
g_N	if((g_n==1.0),exp(-g_s)*(g_s+1), g_n^2*GTFE_sigma(1/g_n)*exp(-g_s)+GTFE_sigma(g_n)*exp(-g_n*g_s))	-
g_J	A_RLD*g_T^2*g_N[A/cm^2]	GTFE current density
g_region	if(g_T>g_T_max,1, if(g_T<g_T_min,-1,0))	Thermal=1, field=-1 or transition=0 (For testing purposes)

Table A.3: COMSOL implementation: main equations.

A.4 Smooth version

The implementation described in table A.3 uses ideal discontinuous Heaviside step functions (*if* conditions). But in computational tasks, smoothed (continuous) Heaviside step functions may be needed. The following table A.4 contains the implementation with ideal step functions replaced with smoothed Heaviside step functions (*flc2hs* in COMSOL).

Name	Expression	Description
g_smooth	5	Smoothness scale of Heavyside step functions (preferably define a comsol parameter for this)
g_scale	min(1/4*(g_T_max-g_T_min), g_smooth)	corrected scale (discontinuations, when >1/4*(Tmax-Tmin))
g_z_s	if(g_T<g_T_min||g_T>g_T_max,0, g_z)	if condition to suppress calculation out of transition region (value might be complex)

g_s_s	flc2hs(g_T-(g_T_max-g_scale), g_scale)*g_B_q+flc2hs((g_T_min+ g_scale)-g_T,g_scale)*g_B_FN+(1-(flc2hs(g_T-(g_T_max-g_scale), g_scale)+flc2hs((g_T_min+g_scale)-g_T,g_scale)))*(g_B_FN+(g_b/2)* g_z_s^2+2/3*g_a*g_z_s^3)	S parameter with Heavyside step functions
g_n_s	flc2hs(g_T-(g_T_max-g_scale), g_scale)*g_beta_T/(g_B_q/g_phi)+ flc2hs((g_T_min+g_scale)-g_T, g_scale)* g_beta_T/(g_C_FN/g_phi)+(1-(flc2hs(g_T-(g_T_max-g_scale), g_scale)+flc2hs((g_T_min+g_scale)-g_T,g_scale)))*1.0	Ratio of energy slope factors
g_N_s	if((g_n_s==1.0),exp(-g_s_s)* (g_s_s+1),g_n_s^2* GTFE_sigma(1/g_n_s)*exp(-g_s_s)+ GTFE_sigma(g_n_s)*exp(-g_n_s* g_s_s))	N parameter
g_J_s	A_RLD*g_T^2*g_N_s[A/cm^2]	GTFE current density (with scaled Heavyside step functions)
g_region_s	flc2hs(g_T-(g_T_max-g_scale), g_scale)*1+flc2hs((g_T_min+ g_scale)-g_T,g_scale)*(-1)	regions with HS

Table A.4: COMSOL implementation: smoothed version.